



MODELING OF LIQUID HYDROCARBON FUEL PRODUCTION FROM PALM OIL VIA CATALYTIC CRACKING USING MCM-41 AS CATALYST

Ivan Yared, Hengky Kurniawan, Nico Wibisono, Yohanes Sudaryanto, Herman Hindarso and Suryadi Ismadji
Department of Chemical Engineering, Faculty of Engineering, Widya Mandala Surabaya Catholic University, Kalijudan, Surabaya, Indonesia

E-mail: suryadiismadji@yahoo.com

ABSTRACT

The objective of this study was to determine the reaction kinetics of the catalytic cracking of palm oil over MCM-41 as a catalyst at the higher C/O ratio and WHSV. The kinetic values obtained from this study can be used further for industrial purpose. In this study, palm oil was cracked using MCM-41 as a catalyst in a fixed bed micro-reactor. The experiment was conducted at the atmospheric pressure, with reaction temperature of 623.15 K, 673.15, and 723.15 K, Weight Hourly Space Velocity (WHSV) of 15, 17.5, 20, 22.5, 25, 27.5, and 30 h⁻¹, and C/O (catalyst/oil) ratio of 1:32.5. The kinetic model used in this study was the three-lump model developed by Weekman, which involves parallel cracking of palm oil to Organic Liquid Product (OLP) and gas plus coke, with consecutive cracking of the OLP to gas plus coke. The model can represent the experimental data fairly well. From the study, the rate constant values k_1 , k_2 , k_3 for reaction temperature of 623.15 K were found to be 9.499, 1.8967 and 0.15565 h⁻¹, respectively. For reaction temperature of 673.15 K, the rate constant values were 20.0674, 3.9725 and 0.6330 h⁻¹. For reaction temperature of 723.15 K, the rate constant values were 28.5494, 5.1498 and 0.6768 h⁻¹. Using the Arrhenius equation, the activation energy is 41.5000, 37.7800 and 12.7437 kJ/mol for E_1 , E_2 , and E_3 , respectively. The pre-exponential factor k_{10} , k_{20} , and k_{30} obtained using the same equations were 30091.6, 2971.14 and 5.82 h⁻¹, respectively.

Keywords: model, palm oil, fuel, production, cracking, liquid hydrocarbon.

INTRODUCTION

Petroleum-based fuel has been in used as a main energy source in human civilization for centuries. Nowadays, the demand of petroleum-based fuel is increasing even more significant than ever because of the rapid growth of industrial and technology. However, since the raw material for the fuel, the petroleum, is a non-renewable resource, this increasing demand would cause the depletion of petroleum reserve. This condition will also lead to other problems, such as escalating crude oil prices and a global energy crisis.

Aside from those future possible problems, the utilization of petroleum-based fuel also has its own disadvantages. Using the petroleum-based fuel would results in a gas emission, such as carbon dioxide, nitrogen, and sulfur compounds. These gases are the main cause for air pollution and green house effect (Kloprogge *et al.*, 2005). Therefore, petroleum-based fuel also gives a great contribution to the global warming.

The scarce of new petroleum resources and environmental problem is caused by the intense use of petroleum-based fuel has lead to the research of alternative fuel as a new energy source replacing the petroleum-based fuel. Biofuel is one of those alternative fuels that currently being studied. Biofuel is defined as liquid or gaseous fuel that can be produced from the utilization of biomass substrates (Ooi *et al.*, 2004a). Vegetable oils can be used as a raw material for an alternative fuel because it is renewable and also free of nitrogen and sulfur compounds (Ooi *et al.*, 2004a, b). Therefore, biofuel obtained from

vegetable oils can be used as a substitute for fuel or fuel additive to reduce gas emission (Twaiq *et al.*, 2003a).

Among all of the vegetable oils available, palm oil is an option that can be used as a raw material for the biofuel (Ooi *et al.*, 2004a, b; Twaiq *et al.*, 2003a, b; Twaiq *et al.*, 2004). Palm oil is one of the most produced vegetable oil in the world, and Indonesia is one of the large palm oil producers in the world with the production capacity is near 15,000,000 tons/year, probably second only to Malaysia. Palm oil is commonly used only as cooking oil and raw material for oleochemical industries (Ooi *et al.*, 2005). At present, several studies have been conducted to convert palm oil into biofuel such as gasoline and diesel fractions through the catalytic cracking of this cooking oil (Ooi *et al.*, 2004a, b; Twaiq *et al.*, 2003a, b; Twaiq *et al.*, 2004). In their study, they used different type of catalysts such as zeolites and other mesoporous silica materials. One of the effective catalyst for the catalytic cracking process are zeolites, such as HZSM-5, as the catalytic cracking over HZSM-5 gave high yield of gasoline fraction (Ooi *et al.*, 2004a,b; Twaiq *et al.*, 2003a, b; Twaiq *et al.*, 2004). The main drawback in using HZSM-5 as a catalyst is the selectivity for gaseous product obtained from the catalytic cracking process which was also high, and it tends to produce more liquid products. Therefore, the mesoporous catalyst MCM-41 can be used as an alternative instead of HZSM-5 to improve the total yield of organic liquid products (OLP) and also production of gasoline range hydrocarbons (Twaiq *et al.*, 2003a, b; Twaiq *et al.*, 2004).



To solve the global energy crisis problem, it is important to bring the laboratory scale production of biofuel to the higher level scale production and if possible to mass production one. However, the C/O (catalyst/oil) ratio used in previous experiments was too high, from 1: 6 to 1: 10, and the yield obtained from those experiments was 67.3% to 98.3%, and the yield of OLP obtained was 42.3% to 62.8% (Ooi *et al.*, 2004a). Even though the high conversion value was obtained, the use of high C/O values are not efficient if this technology be applied in industrial scale since a huge amount of catalyst needed to convert hundred tons of palm oil into liquid hydrocarbon fuel. The conversion of palm oil into liquid hydrocarbon depends on many process parameters such as the type of catalyst, C/O ratio, reaction temperature and WHSVs (weight hourly space velocities). Here we used MCM-41 as the catalyst, since this mesopores material has narrow pore size distribution and ordered pore characteristic. To scale up the catalytic cracking reactor it is necessary to obtain complete feature of the reaction kinetic during the catalytic reaction occurs. This feature usually presented as a reaction model. In the preliminary studies conducted by our other fellows, the product's composition at the optimum C/O ratio and various WHSVs condition at the fixed reaction temperature had been obtained. The optimum C/O ratio was then used to obtain the data of product's composition at various WHSVs and reaction temperature. The main objective of this study is to determine the reaction kinetic of catalytic cracking of palm oil into liquid hydrocarbon fuel.

MATERIALS AND METHODS

MCM-41 synthesis and characterization

The catalyst used in the experiments was prepared using the following methods 2.2778g of hexadecyltrimethyl ammonium bromide (CTAB, Merck) is diluted with 50 ml of water in the glass reactor. 0.0400 g of sodium hydroxide (powder p.a., Merck) is diluted with water to 50ml in volumetric flask. The temperature of reaction is maintained at 80°C by circulating water at desired temperature into the heating jacket of the glass reactor. 5.2159g of tetraethyl orthosilicate (TEOS, 99.8%, Fluka) is added into the reactor under stirring condition. The reagents in the reactor are stirred for 2 hours. The reaction product is then centrifuged for 2 × 10 minutes to obtain the white precipitate. The precipitate is dried using oven at 110°C for 4 hours. Dried product is extracted using ethanol in the glass reactor at 50°C for 24 hours.

To determine the characteristics of the MCM-41, several analyses were conducted. X-ray diffraction (XRD) analysis was conducted on a Rigaku Miniflex Goniometer at 30kV and 15mA using Cu K α radiation; the observation is made at 2 θ angle of 1.5 to 10°. Scanning electron microscopy (SEM) analysis were conducted on a JEOL JSM-6300F using 5 kV accelerating voltage, 7 spot size, 4 aperture, and 15mm working distance. Nitrogen (N $_2$) adsorption/desorption analysis were conducted on a QuadraSorb SI at -194°C after vacuum degassing at 200°C

for 24 hours. Pore size distribution (PSD) is calculated using density functional theory (DFT) using Quadrachrome Quadrawin software with medium regularization.

Catalytic cracking of palm oil

The cracking of palm oil was conducted at atmospheric pressure in a fixed-bed microreactor (150mm × 25mm ID). The oil to catalyst (O/C) ratio was set on 32.5, while the reaction temperatures were varied on 623.15 K, 673.15 K, and 723.15 K with WHSV of 15, 17.5, 20, 22.5, 25, 27.5, and 30 h $^{-1}$. A known amount of MCM-41 catalyst (1.0g) was loaded over 0.2-0.4g of rock wool supported with a stainless steel mesh in a microreactor. The nitrogen gas was introduced into the catalytic cracking apparatus one hour prior to the experiment at the flow rate of 1000 ml/min. The temperatures of the reactor and pre-heater were controlled by a thermocouples placed in the end of horizontal tube (pre-heating section) and catalyst bed. The palm oil was fed into the reactor at certain WHSV (as calculated using equation 1) using a peristaltic pump. Once the maximum run time had been reached (as calculated using equation 2), the collected condensate in the condensate flask was filtered using filter paper Whatman 42. The total mass of liquid product was weighed and the liquid product's composition was analyzed using GC-2014.

$$\text{WHSV} = \frac{\dot{m}_{\text{feed}}}{m_{\text{catalyst}}} \quad (1)$$

$$t_{\text{max}} \text{ (h)} = \frac{\text{O/C}}{\text{WHSV}} \quad (2)$$

Modeling of kinetic catalytic cracking reaction

The data obtained in this experiment are the concentration of UPO (unconverted palm oil), OLP (organic liquid product, including hydrocarbons with chemical formula similar to those of gasoline, kerosene, and diesel), and the side products of the cracking reaction based on the three lumps model previously developed by Weekman, assumed to be gas (including short chain hydrocarbons) and coke. The three-lump model is presented at **Error! Reference source not found.** (Ooi *et al.*, 2004c). These concentration data is presented as weight fraction of the overall product obtained.

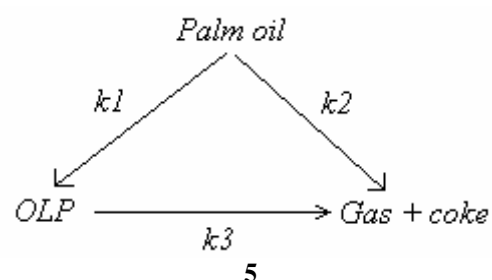


Figure-1. Three-lump kinetic model.



Based on the three-lump model, the cracking rate of the palm oil is defined as follows.

$$-r_{Cp} = -\frac{dCp}{d\tau} = (k_1 + k_2)Cp^n \quad (3)$$

In the present study, the cracking rate of the palm oil is calculated using first order reaction. The rate of products (OLP and gas + coke) formation is defined as follows.

$$\frac{dC_{OLP}}{d\tau} = (k_1Cp - k_3C_{OLP}) \quad (4)$$

$$\frac{dC_{gas+coke}}{d\tau} = (k_2Cp + k_3C_{OLP}) \quad (5)$$

To find the parameters, which are the kinetic rate constants, these equations are solved using least-square method. Using the rate constants and the Arrhenius equation, the value of activation energy and pre-exponential factor for each reaction can be calculated. The experimental data is compared with the estimated data in order to clarify the accuracy of the model. The predicted data is calculated simultaneously using Runge-Kutta method.

Analysis of organic liquid product

OLP was analyzed using gas chromatography (GC-2014). The compositions of OLP were then compared with references of gasoline, kerosene, and diesel (obtained from Pertamina) gas chromatography readings. Using the comparison, the OLP compositions were then calculated.

RESULTS AND DISCUSSIONS

MCM-41 characteristics

The XRD diffractogram obtained from the analysis is shown in **Error! Reference source not found.**. The result shows matching crystalline properties with the MCM-41, with the identical peaks in the hkl indexes of 100, 110, 200, and 210. From the diffractogram, values of d_{100} and a_0 can be calculated using the following equations.

$$d_{100} = \frac{n \cdot \lambda}{2 \cdot \sin \theta} \quad (6)$$

$$a_0 = \frac{2 \cdot d_{100}}{\sqrt{3}} \quad (7)$$

The values of each parameter are $d_{100} = 42.88 \text{ \AA}$ and $a_0 = 49.52 \text{ \AA}$.

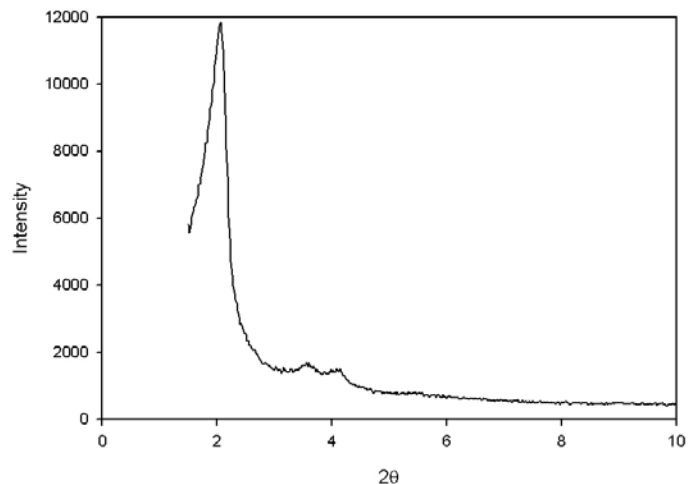


Figure-2. XRD diffractogram of MCM-41 synthesized.

SEM analysis is used to determine the crystalline form and pore array of the material. SEM image obtained from the electron microscopy analysis is shown in **Error! Reference source not found.** The image show the crystalline is consisted of individual silica beads with almost equal bead diameter.

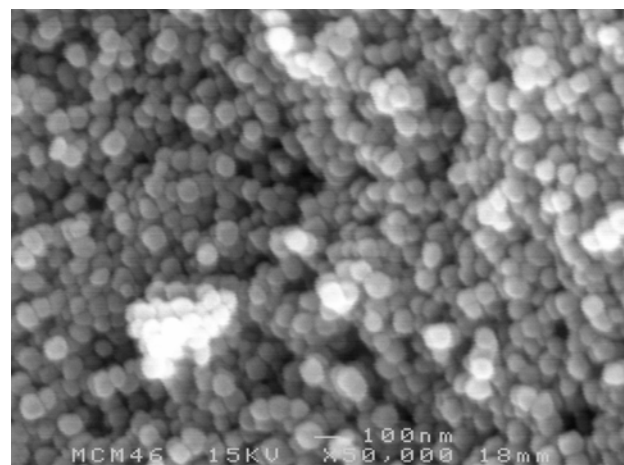


Figure-3. SEM image of MCM-41 synthesized.

The isotherm characteristics are determined using nitrogen sorption analysis. The result is displayed as isotherm curve in **Error! Reference source not found.**. Hysteresis in the isotherm curve shows pores are tubular in shape and open at both ends. This particular specification shows MCM-41 with homogeneous pore distribution.

To determine the pore size distribution, density functional theorem (DFT) is used in the isotherm curve obtained from nitrogen sorption analysis to provide a plot of $dV(r)$ versus pore width as depicted in **Error! Reference source not found.**. The plot shows high peak of $dV(r)$ in the pore size of approximately 33 \AA . This result means that experimental product synthesized is having a uniform pore size. It is also interesting to notice



that the pore width value obtained from PSD curve is lower than a_0 value obtained from calculations based on the XRD result. a_0 value is 49.52 Å while pore width value is approximately 33 Å. From the difference of a_0 value and pore width value, wall thickness of 16.52 Å can be calculated.

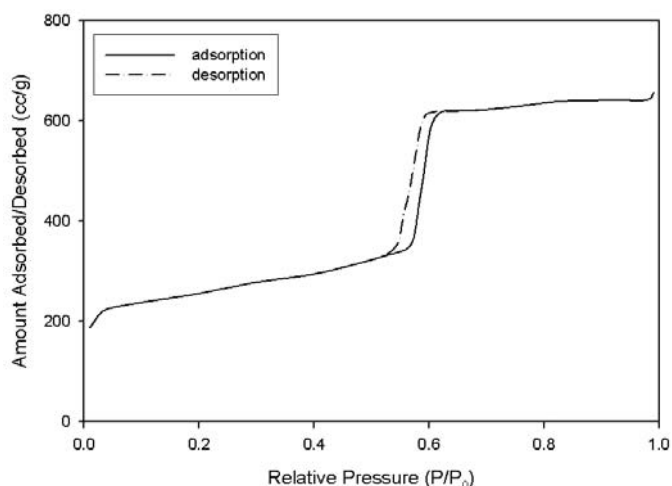


Figure-4. Adsorption/desorption isotherm of MCM-41 synthesized.

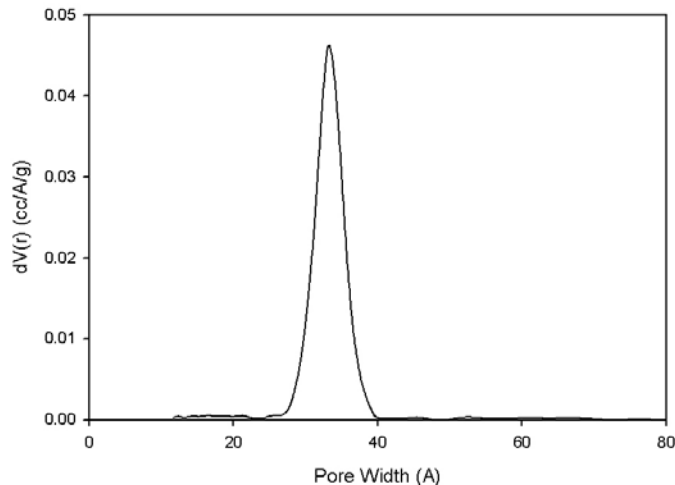


Figure-5. Pore size distribution of MCM-41 synthesized.

Kinetic parameters of catalytic cracking reaction

The experimental data for various reaction temperature and WHSV are presented in **Error! Reference source not found.** It can be observed that the concentrations of the OLP and gas + coke are increasing along with the increase of the reaction temperature, while the concentration of UPO is decreased. In other words, the increase of the reaction temperature is followed by the increase of the total conversion, until the reaction temperature of 723.15 K, the optimum reaction temperature, is used. However, at the lower reaction temperature (623.15 K), the concentration of gas and coke obtained is too low compared to those obtained at higher reaction temperature (673.15 K and 723.15 K). This is assumed to be caused by the secondary cracking reaction, which is not active at lower reaction temperature (Ooi *et al.*, 2004a).

As for the effect of WHSV, **Error! Reference source not found.** also shows that the total conversion is decreased with the increase of WHSV. It is possibly due to the variation of WHSV used in this experiment is higher than the optimum WHSV for the operating condition, because higher WHSV would mean lower residence time and also lowering the chance of the palm oil to be cracked. Although it can be predicted that the optimum WHSV is lower than 15 h⁻¹ (Ooi *et al.*, 2004a), the use of lower WHSV would make the reaction time to be longer and it will be inefficient to be applied at larger scale. Therefore, lower WHSV than 15 h⁻¹ is not used in this experiment.

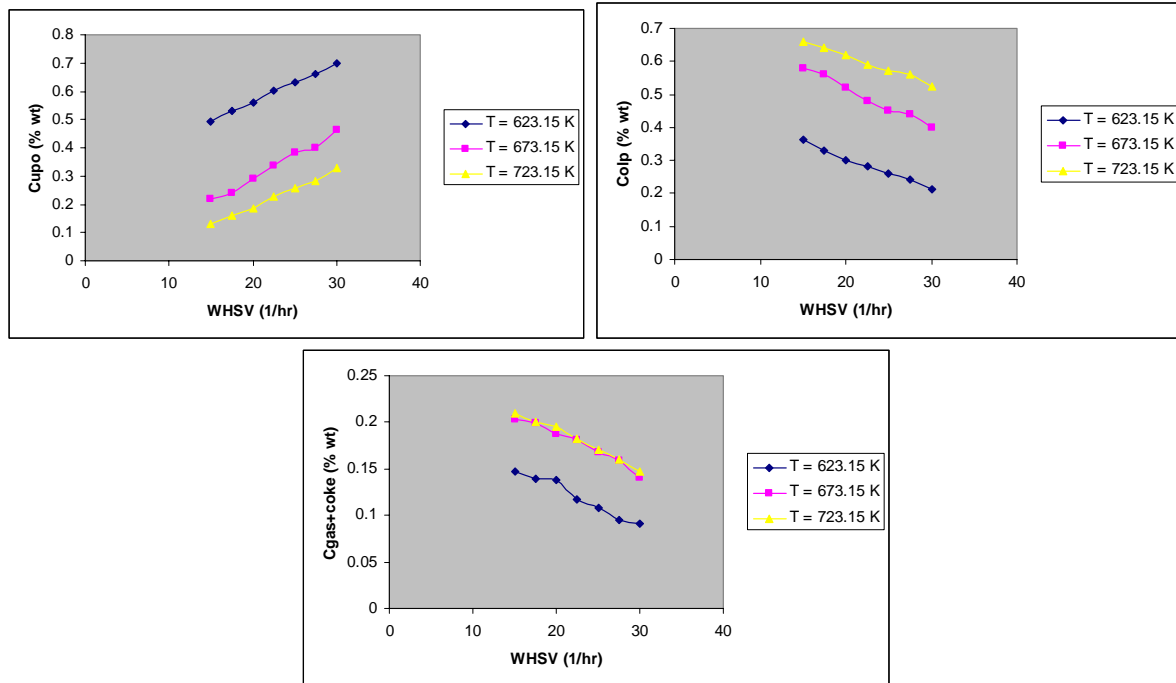


Figure-6. Concentration of UPO (a), OLP (b), and Gas+Coke (c) for Various Reaction Temperatures and WHSV.

Using the equations and method previously described in the kinetic studies, the kinetic constants are found and are presented in Table-1. It can be seen that the kinetic constants are increased with the increase of reaction temperature, especially the OLP formation constant (k_1 value). Compared to these, the increment of another constant value is lower. For gas and coke formation from OLP constant, the value is increased significantly from reaction temperature of 623.15 K to 673.15 K, and the increment is decreased from reaction temperature of 673.15 K to 723.15 K. It can be observed that the secondary cracking reaction happens slightly in lower reaction temperature, and the use of higher temperature would make it to happen a lot more. However, further increase of reaction temperature does not give significant effect to it.

Table-1. Kinetic Constants for Three-Lump Model at Various Reaction Temperatures.

T	623.15 K	673.15 K	723.15 K
k_1 (hr ⁻¹)	9.4990	20.06744	28.5494
k_2 (hr ⁻¹)	1.8967	3.9725	5.1498
k_3 (hr ⁻¹)	0.4837	0.6330	0.6768

The kinetic constant in Table-2 is higher than the constants value found in another experiment. The difference in these values is caused by the difference in the activation energy for each reaction. The activation energy is calculated using the Arrhenius equation with the respective kinetic constants. The activation energy for each reaction in this experiment is lower than the activation energy obtained from literature and another

experiment. The comparison of activation energy obtained in this experiment with the literature data and those obtained in another experiment is presented in Table-2.

Table-2. Comparison of Activation Energies with Gas Oil Cracking from Literatures.

Reaction	E (kJ/mol)		
	Experimental Data	Used Palm Oil (CMZ-40)	Gas Oil
Feed → OLP	41.5	116	42 - 151
Feed → gas + coke	37.78	17	38 - 75
OLP → gas + coke	12.74		54 - 126

The activation energy level is depends on the type of the feedstock and catalyst used. The cracking of gas oil needs higher activation energy because the molecular structure of the compounds in the gas oil different with palm oil. The palm oil contains triglycerides, which very reactive in the present of oxygen in the pore surface of catalyst. The reaction between triglycerides and oxygen creates the carbonium ions on the catalyst, which enable the cracking reaction occurs at lower activation energy (Ooi *et al.*, 2005a). The cracking reaction of feedstock with higher percentage of more-stable saturated fatty acids would need higher activation energy compared to those using feedstock with higher percentage of more-reactive unsaturated fatty acids (Ooi *et al.*, 2005b). The use of MCM-41 would also give different result compared to those using HZSM-5 as a catalyst.



Although HZSM-5 has higher acidity that leads to higher conversion than MCM-41, however the total yield of organic liquid product improved when MCM-41 used as the catalyst. The use of HZSM-5 as the catalyst gave a higher conversion of gaseous product, since this catalyst is more acidic than MCM-41, the secondary cracking of the liquid product into smaller molecules (gases) also increase. MCM-41 has higher selectivity for olefin C_5^+ products than HZSM-5 Juarez *et al.*, 1997).

From Table-2, it can be seen that the activation energy for conversion of palm oil to OLP using CMZ-40 is higher than those of this experiment, and it is an opposite for the activation energy for conversion of palm oil to gas + coke. CMZ-40 is a composite material consists of HZSM-40. The HZSM-40 component in CMZ-40 increase the selectivity for gaseous products and thus lowering the activation energy needed to convert palm oil into gas + coke product. On the contrary, because MCM-

41 has higher selectivity towards liquid products, the activation energy to convert the palm oil to OLP using MCM-41 is lower than those of CMZ-40. The comparison was done based on the fact that the fraction of saturated and unsaturated fatty acids in the used palm oil utilized as feed on the other experiment is similar to those of palm oil used in this experiment.

The experimental data is compared with the estimated data in order to clarify the accuracy of the model. The predicted data is calculated simultaneously using Runge-Kutta method. The graph of experimental data versus estimated data is presented in

Figure-It can be observed from Figure-7 that the deviation between the experimental and predicted data is relatively small. Therefore, this three lump kinetic model is accurate enough and can be used to estimate the experimental result.

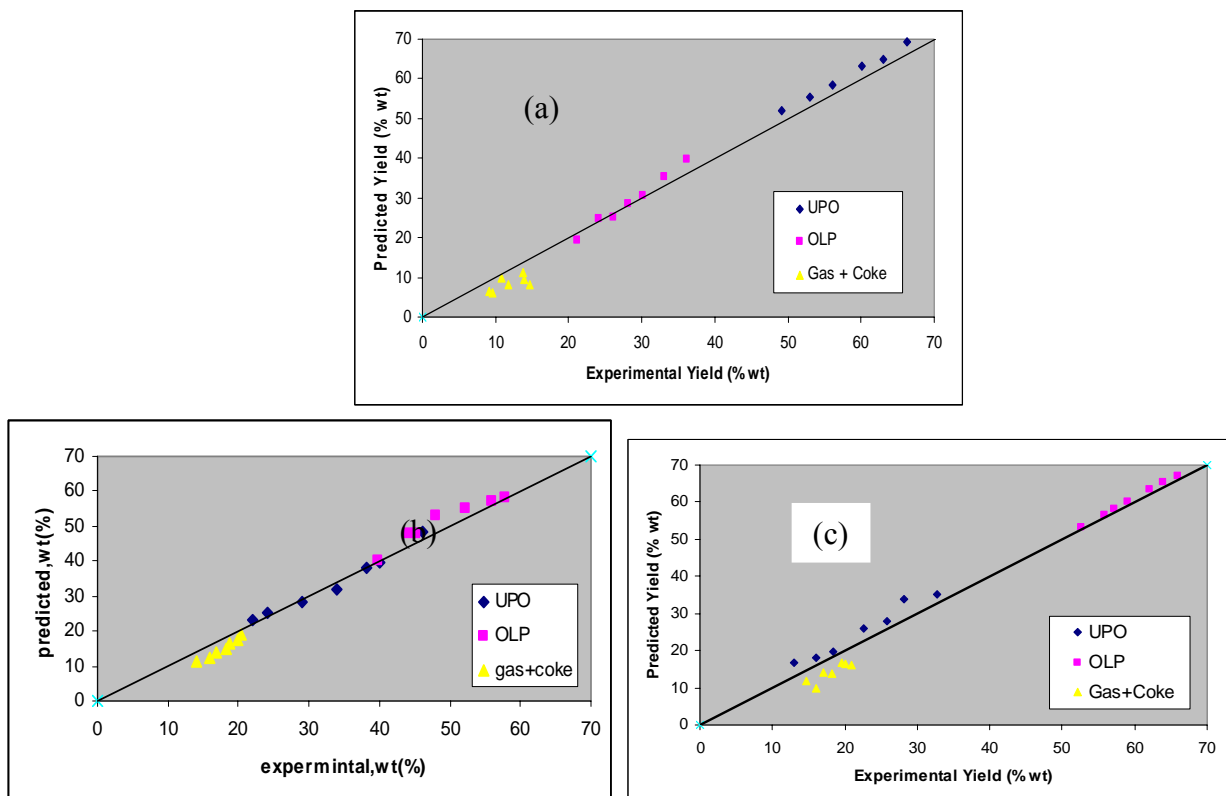


Figure-7. Comparison of Experimental Concentration Yield of UPO, OLP, and Gas+Coke with the Predicted Ones for Reaction Temperature of 623.15 K (a), 673.15 K (b) 673.15, (c) 723.15 K.

REFERENCES

Juarez J.A., Isunza F.L, Rodriguez E.A. and Mayorga J.C.M. 1997. A Strategy for Kinetic Parameter Estimation in The Fluid Catalytic Cracking Process. *Ind. Eng. Chem. Res.* 36: 5170-5174.

Klopogge J.T, Duong L.V, Frost R.L. 2005. A Review of the Synthesis and Characterisation of Pillared Clays and

Related Porous Materials for Cracking of Vegetable Oils to Produce Biofuels. *Environ. Geol.* 47: 967-981.

Ooi Y.S., Zakaria R., Mohamed A.R., Bhatia S. 2004a. Catalytic Conversion of Palm Oil-Based Fatty Acid Mixture to Liquid Fuel. *Bimass Bioenergy.* 27: 477-484.

Ooi Y.S., Zakaria R., Mohamed A.R., Bhatia S. 2004b. Synthesis of Composite Material MCM-41/Beta and Its



www.arpnjournals.com

Catalytic Performance in Waste Used palm Oil Cracking.
Applied Catalysis A: General. 274: 15-23.

Ooi Y.S., Zakaria R., Mohamed A.R., Bhatia S. 2005a.
Catalytic Conversion of Fatty Acids Mixture to Liquid
Fuels over Mesoporous Materials. *React. Kinet. Catal.
Lett.* 84: 295-302.

Ooi, Y.S., Zakaria, R., Mohamed, A.R., Bhatia, S., 2004c.
Catalytic Cracking of Used Palm Oil and Palm Oil Fatty
Acids Mixture for the Production of Liquid Fuel: Kinetic
Modeling. *J. Am. Chem. Soc.*, 18, 1555-1561.

Ooi Y.S., Zakaria R., Mohamed A.R., Bhatia S., 2005b.
Catalytic Conversion of Fatty Acids Mixture to Liquid
Fuel and Chemicals over Composite Microporous/
Mesoporous Catalysts. *J. Am. Chem. Soc.*, 19: 736-743.

Twaiq F.A., Mohamed A.R., Bhatia S. 2003a. Liquid
Hydrocarbon Fuels from Palm Oil by Catalytic Cracking
over Aluminosilicate Mesoporous Catalysts with Various
Si/Al Ratios. *Microporous Mesoporous Mater.* 64: 95-107.

Twaiq F.A., Zabidi N.A.M., Mohamed A.R., Bhatia S.
2003. Catalytic Conversion of Palm Oil over Mesoporous
Aluminosilicate MCM-41 for the Production of Liquid
Hydrocarbon Fuels. *Fuel Process. Technol.* 84: 105-120.

Twaiq F.A.A., Mohamad A.R., Bhatia, S. 2004.
Performance of Composite Catalysts in Palm Oil Cracking
for the Production of Liquid Fuels and Chemicals. *Fuel
Process. Technol.* 85: 1283-1300.